



Novel role of cholesteryl ester transfer protein (CETP): attenuation of adiposity by enhancing lipolysis and brown adipose tissue activity

Helena F. Raposo^{a,b}, Patricia Forsythe^a, Bruno Chausse^b, Júlia Z. Castelli^{a,b}, Pedro M. Moraes-Vieira^{b,c,d}, Valéria S. Nunes^e, Helena C.F. Oliveira^{a,b,*}

^a Department of Structural and Functional Biology, Institute of Biology, State University of Campinas, Campinas, SP, Brazil

^b Obesity and Comorbidities Research Center, Institute of Biology, State University of Campinas, Campinas, SP, Brazil

^c Laboratory of Immunometabolism, Department of Genetics, Evolution, Microbiology and Immunology, Institute of Biology, State University of Campinas, Campinas, SP, Brazil

^d Experimental Medicine Research Cluster (EMRC), State University of Campinas, SP, Brazil

^e Laboratório de Lipídeos (LIM10), Hospital das Clínicas HCFMUSP, Faculdade de Medicina, Universidade de São Paulo, São Paulo, SP, Brazil

ARTICLE INFO

Article history:

Received 29 July 2020

Accepted 4 November 2020

Keywords:

CETP
Adiposity
Lipolysis
Oxygen consumption
Brown adipose tissue

ABSTRACT

Objective: The systemic function of CETP has been well characterized. CETP plasma activity reduces HDL cholesterol and thus increases the risk of atherosclerosis. Here, we investigated whether CETP expression modulate adiposity.

Methods: Body adiposity and energy metabolism related assays and gene/protein expression were compared in CETP transgenic and non-transgenic mice and in hamsters treated with CETP neutralizing antibody.

Results: We found that transgenic mice expressing human CETP present less white adipose tissue mass and lower leptinemia than nontransgenic (NTg) littermates. No differences were found in physical activity, food intake, fat fecal excretion, lipogenesis or exogenous lipid accumulation in adipose depots. Nonetheless, adipose lipolysis rates and whole-body energy expenditure were elevated in CETP mice. In accordance, lipolysis-related gene expression and protein content were increased in visceral and brown adipose tissue (BAT). In addition, we verified increased BAT temperature and oxygen consumption. These results were confirmed in two other animal models: 1) hamsters treated with CETP neutralizing antibody and 2) an independent line of transgenic mice expressing simian CETP.

Conclusions: These findings reveal a novel anti-adipogenic role for CETP.

© 2020 Elsevier Inc. All rights reserved.

1. Introduction

CETP is a 74-kDa glycoprotein expressed in several tissues, including adipose tissue and liver [1]. Primates, rabbits, hamsters, reptiles and fishes express CETP, while mice, rats and dogs do not [2,3]. In humans, CETP is highly expressed in adipose tissue, and its expression is higher in small adipocytes with lower lipid content [4]. Once

Abbreviations: CETP, cholesteryl ester transfer protein; hCETP, human CETP transgenic mice; sCETP, simian CETP transgenic mice; NTg, non-transgenic mice; TG, triglycerides; CHOL, total cholesterol; NEFA, nonesterified fatty acids; Apo, apolipoprotein; FT4, Free thyroxine; CS, citrate synthase; iBAT, interscapular brown adipose tissue; pWAT, white perigonadal adipose tissue (pWAT); EE, whole-body energy expenditure; ATGL, adipose triglyceride lipase; B3AR, beta-3 adrenergic receptor; HSL, hormone sensitive lipase; UCP1, uncoupling protein 1; FATP1, fatty acid transport protein 1; PRDM16, PR domain containing 16; Cidea, cell death inducing DFFA like effector A; Zfp516, zinc finger protein 516; PPAR γ , peroxisome proliferator-activated receptor gamma; PGC1 α , PPAR γ coactivator 1- α ; LPL, lipoprotein lipase; SREBP-1c, sterol regulatory element-binding protein 1; NNT, nicotinamide nucleotide transhydrogenase.

* Corresponding author at: Instituto de Biologia, Universidade Estadual de Campinas, Rua Carl Von Linnaeus, Bloco Z, Campinas, SP CEP 13083-864, Brazil.

E-mail address: ho98@unicamp.br (H.C.F. Oliveira).

in the blood circulation, CETP mediates the exchange of esterified cholesterol from HDL for triglycerides (TG) from apolipoprotein B-containing lipoproteins [5]. The net lipid flux results in a reduction in HDL cholesterol, and because of that, CETP is thought to increase the risk of cardiovascular disease. Thus, in recent decades, the pharmacological inhibition of CETP has been postulated as an anti-atherogenic therapy. At least four CETP inhibitors have gone into clinical trials. Despite initial major setbacks in clinical trials due to increased mortality [6] or futility [7,8], the recent anacetrapib REVEAL trial showed a significant reduction in the incidence of major coronary events [9]. Thus, the hypothesis that CETP inhibitors are anti-atherogenic in humans is still being tested [10].

In addition to its activity in modulating plasma lipoprotein metabolism, CETP may also be important for lipid homeostasis in adipocytes. Previous studies reported that CETP stimulates the selective uptake of HDL cholesteryl esters by human isolated adipocytes [11] and by several tissues in CETP transgenic mice, including adipose tissue [12]. In addition, it was previously demonstrated that CETP overexpression in liposarcoma SW872 cells increases TG hydrolysis, reduces TG synthesis and thus reduces TG content [13].

Numerous genes have been shown to modulate adiposity during recent decades. Among them, genes encoding proteins primarily related to plasma lipoprotein transport have been associated with body fat accumulation, such as apolipoprotein (apo) CIII and apo E [13–16]. In a previous work, we demonstrated that CETP expression attenuated diet-induced obesity in hypertriglyceridemic apo CIII-overexpressing mice [17]. Thus, in this study, we aimed to evaluate the impact of whole-body CETP expression on adiposity and disclose the underlying mechanisms.

2. Material and methods

2.1. Animal studies

All animal protocols were approved by the State University of Campinas Committee for Ethics in Animal Experimentation (CEUA – UNICAMP, #1607-1, #3279-1, #3870-1, #5122-1/2019). Two independent lines of CETP transgenic mice were used: hCETP - heterozygous human CETP transgenic mice (line 5203) expressing a natural promoter-driven human CETP transgene [18]; and sCETP - overexpressing a metallothionein promoter-driven simian CETP cDNA (C57BL/6-Tg(CETP)UCTP20Pnu/J) [19]. The hCETP line was kindly provided by Dr. Alan Tall from Columbia University (NY, EUA) in 1996, and the sCETP line was purchased from The Jackson Laboratory (Bar Harbor, USA) in 2013. Both colonies were then maintained as heterozygous by crossing with C57BL/6JUnib mice from State University of Campinas Multidisciplinary Center for Biological Research in Laboratory Animals (CEMIB/Unicamp, Brazil). Experiments were performed in five-month-old female mice, although initial studies were performed in male mice (Fig. S1), with similar results. Their respective nontransgenic littermates (NTg) were used as controls. Mice were genotyped according to the protocols recommended by the Jackson Laboratory (<https://www.jax.org>). Total cholesterol (Table 1) and HDL-cholesterol plasma levels are reduced in CETP expressing mouse lines as previously reported and shown in Supplementary Table S1.

Golden Syrian hamster, a natural CETP-expressing species, was also used. One-month-old female hamsters were purchased from the Medical School of São Paulo University, Brazil. They were randomly assigned to control or experimental (CETP inhibition) groups. For 4 weeks, hamsters received a monoclonal anti-CETP (TP2) antibody (donated by Dr. Alan Tall, Columbia University, NY, EUA) subcutaneously three times a week (25 µg/kg) or irrelevant antibody (IgG nonimmunogenic, Sigma Chemical Co.) as a control [20]. Antibodies were previously purified in a detoxification column (Affinity Pak Detoxi-Gel, Pierce, Rockford, EUA). Animals were maintained under controlled temperature (22 ± 2 °C) in a 12-h light/dark cycle in conventional animal facility (3–5 mice/cage), with wood shavings bedding and free access to filtered water and regular rodent diet (Nuvital CR1, Colombo, PR, Brazil). The number of mice varied from 6 to 12 per group according to the variance of the data for each protocol, and the exact number

Table 1
Plasma levels of lipids and glucose of human (hCETP) and simian (sCETP) CETP transgenic mice and respective nontransgenic (NTg) littermates.

	NTg	hCETP	NTg	sCETP
Glucose (mg/dL)	91.5 ± 3.1	100.9 ± 4.6	181.1 ± 16.8	169.3 ± 9.11
CHOL (mg/dL)	92 ± 6	76 ± 5***	103.5 ± 4.4	71.9 ± 4.9***
TG (mg/dL)	93 ± 5	99 ± 8	131.0 ± 9.2	137.5 ± 6.0
TBA (µM)	23.3 ± 1.2	24.6 ± 2.2	28.0 ± 4.6	24.4 ± 4.8

Mean ± SE (n = 6–11 hCETP and NTg, fasting plasma; n = 6–7 sCETP and NTg, fed plasma). CHOL, cholesterol; TG, triglycerides; TBA, total bile acid. Student's *t*-test, ****p* < 0.001.

used is provided in the legend of the figures. Animals were anesthetized for terminal experiments with ketamine (100 mg/kg) and xylazine (10 mg/kg) ip, followed by exsanguination through the retro-orbital plexus. All animal experiments were performed between 8:00 and 11:00 pm.

2.2. Physical activity

Two independent methods for physical activity were used. For voluntary physical activity, mice had free access to an individual running wheel for 7 days in individual cages. The revolutions of each running wheel were recorded within 5-min intervals (Columbus Instruments, OH, USA). Data are presented as the daily mean distance traveled. The second method was an infrared cage system (Phecomp System, Panlab Harvard Apparatus) to measure total spontaneous activity (all movements): mice were placed in cages with free access to food and water for 24 h, and animal activity and rearing were recorded simultaneously by the means of 2-dimensional infrared frames.

2.3. Temperature

Body (rectal) temperature was measured using a thermometer with a probe for mice (RET-3 Physitemp), and the FLIR T450sc thermosensitive camera (FLIR Systems, Inc. Wilsonville, USA) was used for specific body regions (interscapular brown adipose tissue - iBAT).

2.4. Indirect calorimetry

The Oxylet System (Pamlab e Harvard Apparatus) was used for indirect calorimetry. hCETP mice were adapted to the chamber twice for 15 min and acclimated for 10 min immediately before the measurements. Then, two measurements were performed in 12-h-fasted mice between 9:00 am and 12:00 pm. sCETP transgenic mice were acclimated to the chamber for 24 h, and the air gases were measured during the next 24 h. Mice had free access to food and water. The software Metabolism v2.2.01 was used to calculate total energy expenditure (EE). In separate experiments, oxygen consumption (VO₂) was also evaluated in response to intraperitoneal injection of isoproterenol (10 mg/kg BW) in anesthetized mice (ketamine, 100 mg/kg and xylazine, 10 mg/kg).

2.5. Carcass composition

The carcasses were dehydrated at 65 °C until body weight stabilized (dry weight). The total fat was then extracted with petroleum ether (LabSynth, SP, Brazil) in a Soxhlet extractor for 72 h. The fat mass is calculated by the weight difference of the dehydrated carcass before and after lipid extraction. Lean mass corresponds to the weight of dehydrated and delipidated carcasses.

2.6. Whole-body adipose volume – micro computerized tomography

Anesthetized mice were placed in the micro-CT scanner (Bruker - Skyscan 1178). The energy parameters (49 kV; 402 µA; 20 W) were set as previously reported [21]. The images were obtained in duplicate, 180°, grayscale and 84 µm resolution. The region of interest (from cervical to coccyx) was determined according to the bone projections, and the lung was excluded from each image. The 2D images were reconstructed with NRecon software (Feldkamp algorithm). Then, images were binarized to black and white according to the established threshold, and the object volume (total adipose tissue volume) was calculated by CT Analyser, Version: 1.13.5.1, according to the Bruker instructions manual.

2.7. Plasma biochemical analyses

The plasma levels of total cholesterol (CHOL), triglycerides (TG) (Chod-Pap; Roche Diagnostic GmbH, Mannheim, Germany), nonesterified fatty acids (NEFA) (Wako Chemicals, Neuss, Germany) were determined using enzymatic colorimetric assays according to the manufacturer's instructions. Leptin and adiponectin plasma concentrations were determined by ELISA kits (Merck Millipore, Darmstadt, Germany). Free thyroxine (FT4) was determined by an ELISA kit (Cloud-corp, Katy, USA). Corticosterone was analyzed using an ELISA kit (Cayman Chemical, Ann Arbor, USA). Epinephrine and norepinephrine were analyzed by a research enzyme immunoassay (ELISA) kit from LDN, Nordhorn, Germany. Plasma total bile acids were determined using an enzymatic-colorimetric assay kit from Cell Biolabs, San Diego, USA.

2.8. Adipocyte isolation and tissue histology

Adipocytes from fed mice were isolated according to a modified protocol for rat adipocytes [22]. Briefly, perigonadal and subcutaneous fat were digested at 37 °C with collagenase II (Sigma-Aldrich, St. Louis, MO) (1 mg/mL) in Krebs-Ringer bicarbonate buffer (KRBA) with fatty-acid-free albumin (3%) and glucose (6 mM) at pH 7.4 for 45 min under continuous gentle shaking. Cells were filtered through a nylon mesh and washed 3 times with KRBA buffer to eliminate the stroma-vascular fraction and collagenase. Isolated adipocytes were used for lipogenesis and lipolysis assays. In addition, adipose tissue depots were also submitted to conventional histological analysis. Briefly, adipose depots were fixed with 4% paraformaldehyde during 24 h at 4 °C, washed with PBS and preserved in ethanol 70%. Samples were then dehydrated in ethanol, and then transferred to xylene solution for embedding in paraffin. Five-micrometer sections were cut in a Leica microtome. Slides were placed at 70 °C to remove paraffin. Sections were stained with eosin-hematoxylin and digital images were captured under 40× objective lens in an optical microscope (Olympus BX51, camera Olympus U-TVO.63XC). The area of at least 100 WAT adipocytes per section, in 5 different sections per mice, were measured using Image J version 1.53a software. iBAT lipid content was measured with the automated mode after binary transformation within a fixed area/section, five sections/mouse.

2.9. Lipogenesis rates in isolated adipocytes

Isolated adipocytes (10^6 cells) from fed mice were incubated in triplicate in Krebs-Ringer phosphate buffer containing 3% fatty-acid-free BSA, 6 mM glucose, 1 mM acetate and 25 μ U human insulin for 2 h at 37 °C and saturated with a gas mixture of CO₂ (5%)/O₂ (95%) in a shaking water bath. All samples were incubated with 1 μ Ci of ¹⁴C-acetate (GE Healthcare-Amersham, United Kingdom). After incubation, lipids were extracted according to Dole's protocol. Briefly, 0.2 mL of H₂SO₄ (8 N) was added to the samples, and after a 30-min incubation, the reaction mixture was treated with 2.5 mL of Dole's reagent (isopropanol: n-heptane: H₂SO₄, 4:1:0.25, v/v/v). Beta radiation in the lipid extract was counted with scintillation liquid (GE Healthcare-Amersham, United Kingdom) in a Beckman - LS 6000TA Beta counter.

2.10. Lipolysis rates in isolated adipocytes

Glycerol release rates from adipocytes to media were measured as indicators of lipolysis. Isolated adipocytes (10^6 cells) from fed mice were incubated in triplicate with Krebs-Ringer phosphate buffer containing 3% fatty-acid-free BSA and 6 mM glucose, pH 7.4, for 1.5 h at 37 °C in the presence of isoproterenol (10^{-5} M), a beta-adrenergic receptor agonist. A preincubation of 5 min with adenosine deaminase

(0.2 U/mL) at 37 °C was performed. The glycerol content of the incubation medium was measured using an enzymatic-colorimetric assay (Bioclin, Quibasa; BH, Brazil).

2.11. In vivo lipolysis

Lipolysis was estimated as the plasma glycerol concentration in the basal condition and after isoproterenol stimulation. Plasma samples were collected from the tail tip of fed mice before and 15 min after isoproterenol ip injection (0.3 mg/kg) [23]. The plasma glycerol concentrations were measured using an enzymatic-colorimetric assay (Bioclin, Quibasa; BH, Brazil).

2.12. In vivo lipogenesis

De novo lipid synthesis was measured by ³H₂O incorporation into total lipids in the liver and adipose tissues [24]. Mice were injected with ³H₂O (20 mCi; intraperitoneal) in saline solution and killed after 1 h. Lipid tissues were extracted by the Folch method and beta radiation was counted with scintillation liquid (GE Healthcare-Amersham, United Kingdom) in a Beckman - LS 6000TA Beta counter. Plasma was used to determine the specific activity, and the results are expressed as nmol ³H₂O/h/g tissue.

2.13. Exogenous lipid retention capacity

Mice (8 h fasted) received an oral dose of ³H-triolein (5 μ Ci 3H-TO, GE Healthcare-Amersham, United Kingdom) mixed with corn oil (180 mg/mouse). After 24 h, mice were killed and liver, gastrocnemius muscle and perigonadal, subcutaneous and interscapular brown fat depots were excised and weighed. Tissue lipids were extracted using the Folch method and beta radiation was counted with scintillation liquid (GE Healthcare-Amersham, United Kingdom) in a Beckman - LS 6000TA Beta counter.

2.14. Citrate synthase activity

The citrate synthase (CS) activity assay was based on the original protocol from Shepherd and Garland [25], where the conversion of oxaloacetate and acetyl-CoA to citrate and SH-CoA catalyzed by CS is monitored by the colorimetric product thionitrobenzoic acid.

2.15. iBAT mitochondria isolation

Interscapular BAT (iBAT) depots were pooled from 3 mice and placed in ice-cold medium 1 containing 250 mM sucrose, 10 mM HEPES and 1 mM EGTA. Preparations from wild-type and sCETP transgenic mice were made and run in parallel. The BAT was finely minced with scissors and homogenized in a Potter homogenizer. Throughout the isolation process, tissues were kept on ice. Mitochondria were isolated by differential centrifugation. BAT homogenates were centrifuged at 8500 \times g for 10 min at 4 °C. The resulting supernatant, containing floating fat, was discarded. The pellet was resuspended in ice-cold medium 1. The resuspended homogenate was centrifuged at 800 \times g for 10 min, and the resulting supernatant was centrifuged at 8500 \times g for 10 min. The resulting mitochondrial pellet was resuspended in ice-cold medium 2 containing 100 mM KCl, 20 mM Hepes (pH 7.2), 1 mM EDTA, and 0.6% fatty-acid-free BSA and centrifuged at 8500 \times g for 10 min. The final mitochondrial pellets were resuspended in the same medium. The concentration of mitochondrial protein was measured using the Bradford method with BSA as the standard. Procedure adapted from Shabalina et al. [26].

2.16. iBAT mitochondrial oxygen consumption

Oxygen consumption rates were monitored using a Clark-type oxygen electrode coupled to a high-resolution Oroboros respirometry

system at 37 °C [27]. Brown-fat mitochondria (0.0625 mg protein/mL) were incubated in a medium consisting of 125 mM sucrose, 20 mM Hepes (pH 7.2), 2 mM MgCl₂, 1 mM EDTA, 4 mM KH₂PO₄, and 0.1% fatty-acid-free BSA. The respiratory activity of mitochondria was measured in the presence of 5 mM pyruvate plus 3 mM malate. UCP1-linked respiration was measured as the difference between the initial respiration rate (basal) and the residual respiration following the addition of 1 mM GDP. Maximal oxygen consumption rates were obtained by the addition of CCCP to a final concentration of 5 μM.

2.17. iBAT biopsy oxygen consumption rates

Briefly, tissue explants (3–4 mg) were incubated in DMEM (25 mM glucose, 2 mM glutamine, 1 mM pyruvate) supplemented with 4% fatty-acid-free BSA (w/v). Oxygen consumption rates were monitored using a Clark-type oxygen electrode coupled to a high-resolution Oroboros respirometry system at 37 °C under continuous stirring [27,28]. Recordings after 10 min of the experiment (5-min window), when respiration rates were stable, were analyzed and normalized by tissue weight.

2.18. Gene expression analysis

Adipose tissue RNA was extracted from 100 mg of tissue using the RNeasy Lipid Tissue Mini Kit (QIAGEN, Germany) according to the manufacturers' instructions. The RNA integrity was evaluated using Tris-borate 1.2% agarose gels stained with GelRed Nucleic Acid Gel Stain (Biotium). The amount and purity of the RNA were determined by optical density readings at 260 and 280 nm (NanoVue Plus Spectrophotometer, GE Healthcare). Genomic DNA contamination was ruled out by running a polymerase chain reaction (PCR) on the RNA samples. Reverse transcription into cDNA was performed using 2 μg of RNA by reverse transcription using an Applied Biosystems kit (High-Capacity cDNA reverse transcription kit) according to the manufacturer's instructions. Real-time RT-PCR was carried out on a sequence detection system (7500 fast Real-time PCR System, Applied Biosystems, Foster City, CA, USA) using a SYBR Green PCR master mix and specific primer sequences shown in Table S2 (Supplemental material). The cycle thresholds of genes of interest were normalized to β-actin levels by the ΔΔCt method.

2.19. Western blot

Adipose tissue samples were homogenized in urea lysis buffer (2 M thiourea, 5 mM EDTA, 1 mM sodium fluoride, 1 mM sodium orthovanadate, 1 mM sodium pyrophosphate, 1% aprotinin, 2 mM PMSF, and 1% Triton-X 100), and protein concentrations were determined using the Bradford method. Fifty-microgram samples of protein lysate were resolved on 10% SDS-polyacrylamide gels and transferred to nitrocellulose membranes. The membranes were blocked with 5% albumin in Tris-HCl, pH 7.6, containing 150 mM sodium chloride and 0.1% Tween-20 (TBST) and incubated for 2 h at room temperature with primary antibodies against HSL and pHSL (1:1000, Cell Signaling #4107, #4126) and UCP1 (1: 500, Santa Cruz Biotechnology #6529). An antibody against tubulin was used as an internal control (1:30,000, Sigma #T6074).

2.20. Adipose tissue macrophage phenotyping by flow cytometry

Perigonadal adipose stromal vascular fraction was resuspended in PBS containing 2% FBS and stained with saturating concentrations of fluorescent monoclonal antibodies for surface markers. Intracellular staining was performed followed a 5 h *in vitro* stimulation at 37 °C under 5% CO₂ using a leukocyte activation cocktail (BD Biosciences)

as previously described [29]. Cells were permeabilized using the BD kit Cytofix/Cytoperm Fixation/Permeabilization kit as recommended by the manufacturer (BD Biosciences). Data were acquired in FACS Galios (Beckman Counter) and analyzed with the software FlowJo 9.5.3 (TreeStar). The following monoclonal antibodies were used: F4/80 (Cl:A3-1, Biolegend), IL-1β (NJTEN3, eBioscience), TNF (MP6-XT22, Biolegend), CD11c (N418, Biolegend), CD206 (C068C2, Biolegend).

2.21. Adipose tissue cholesterol content by GCMS

Cholesterol content was determined by gas chromatography coupled with mass spectrometry (GCMS) (Shimadzu GCMS-QP2010 plus, Kyoto, Japan), using the software GCMS solution, version 2.5. Lipids were extracted with chloroform:methanol (2:1). The internal standard 5-α-cholestane was added to the lipid extracts and then subjected to saponification with 1 mL of 1 M KOH (dissolved in ethanol) at 60 °C for 1 h. One mL of water was added, and the mixture was extracted twice with hexane. The hexane phase was dried under nitrogen and derivatized with 200 μL of a solution containing pyridine (100 μL) and BSTFA with 1% TMCS (1:1, v/v) (100 μL) and incubated 1 h at 60 °C. One microliter was then injected into the GC-MS with a split rate of 1:3. The sterol separation was achieved in a Restek capillary column (100% dimethyl polysiloxane-Rxi13323) that was 30 m long with an internal diameter of 0.25 mm, contained helium as the mobile phase, and had a constant linear velocity of 45.8 cm/s with an oven temperature maintained at 280 °C. The mass spectrometer operated on the electron impact mode at an ionization voltage of 70 eV with a source temperature of 300 °C for the ions and the interface. Ions were monitored at SIM mode (single ion monitoring). The selected ions were $m/z = 217, 149$ e 109 for 5-α-cholestane and $m/z = 121, 129$ e 329 for cholesterol. The quantitation was based on the total ions chromatogram (TIC) and the identification was based on the comparison with the retention times and mass spectra of standards with correction for the internal standard and tissue mass [30].

2.22. Cold exposure

NTg and sCETP mice (female, 5-month-old) were exposed to cold (4 °C) for 24 h, singly caged, no bedding, in a 12 h light/dark cycle. No food was offered during the first 6 h but with free access to chow diet thereafter. Body temperature (rectal temperature) was measured every 2 h during the first 6 h and at the end of 24 h.

2.23. Statistical analyses

The results are presented as the mean ± standard error for the number of determinations (n) indicated. Student's *t*-test was used for two-group comparisons and two-way ANOVA with Bonferroni posttest for spontaneous physical activity. Statistical significance was defined as $p \leq 0.05$.

3. Results

3.1. CETP expression reduces adiposity

To investigate the effect of CETP on adiposity, we studied heterozygous transgenic mice for the human CETP (hCETP) minigene under the control of its natural promoter compared with their nontransgenic (NTg) littermates. The study was performed in females because initial experiments showed a more prominent reduction in white visceral adipose tissue in female hCETP mice than in males (22% vs 52% in males and females, respectively, Fig. S1B vs Fig. 1B). Although body weight is not modified by CETP expression (Fig. 1A, B), adipose mass is reduced

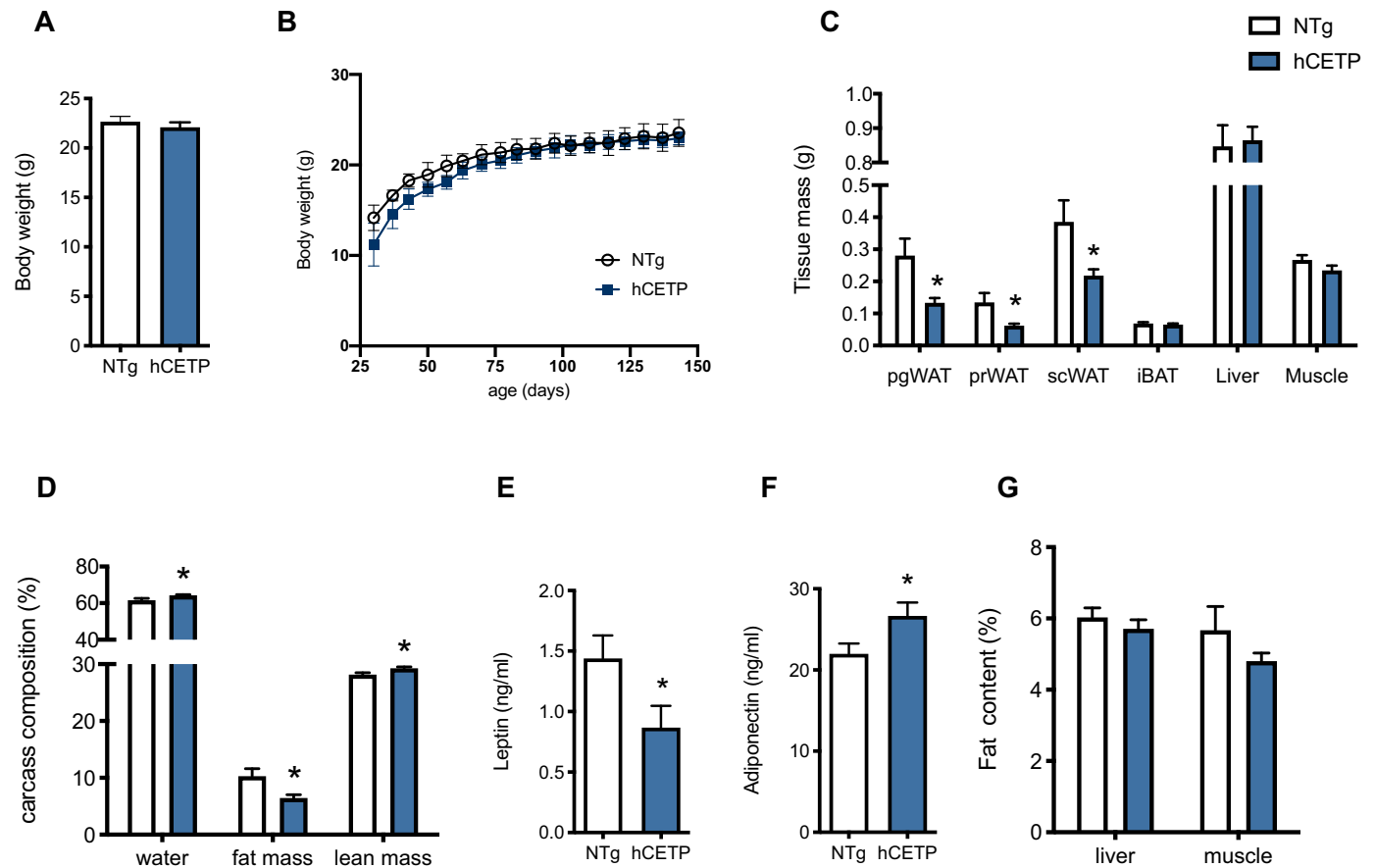


Fig. 1. CETP expression reduces adiposity. (A) Body weight (B) body weight gain and (C) tissue mass: perigonadal (pgWAT), perirenal (prWAT), subcutaneous (scWAT), interscapular brown (iBAT) adipose tissue; liver and gastrocnemius muscle ($n = 8-10$); (D) carcass composition ($n = 10$); (E) leptin ($n = 10-11$) and (F) adiponectin ($n = 11-12$) plasma levels; and (G) liver and skeletal muscle fat content ($n = 7$) of nontransgenic (NTg) and human CETP (hCETP) mice. Mean \pm SE. Student's t-test, * $p \leq 0.05$.

by ~50% in perigonadal and perirenal depots and by ~40% in inguinal subcutaneous adipose tissue (Fig. 1C). In terms of carcass composition, relative lean mass is increased by 4% and relative fat mass is decreased by 37% (Fig. 1D). Consistently, plasma levels of the adipokines leptin and adiponectin were decreased (40%) and increased (20%), respectively, in hCETP mice (Fig. 1E, F). We also show that there is no evidence of ectopic lipid deposition in the liver and muscle (gastrocnemius) of the hCETP mice, since both groups show similar fat contents in these tissues (Fig. 1G). Morphology and adipocyte areas of WAT and iBAT are shown in Supplementary Fig. S2. hCETP pgWAT adipocytes area is decreased compared to NTg adipocytes, while iBAT lipid content is similar between groups.

To verify whether these data were a feature of this particular transgenic mouse model, we immunologically inhibited CETP in a natural CETP-expressing species, the Golden Syrian hamster. One-month-old female hamsters were injected subcutaneously three times a week with the monoclonal antibody anti-CETP (TP2) or irrelevant antibody (nonimmunogenic IgG) for one month. The antibody accomplished potent *in vivo* inhibition of plasma CETP activity (Fig. 2A). CETP immunological inhibition did not change body weight gain or body weight (Fig. 2B, C) but increased perigonadal adipose mass (Fig. 2D, 40%) and adipocyte area (Fig. 2E, 30%).

3.2. Exclusion of possible mechanisms responsible for differential adiposity in CETP-expressing mice

We investigated the eating and activity behavior of hCETP and NTg mice but verified no significant differences in food intake, fat

excretion, stimulated physical activity (running wheel in the cage), or rectal temperature (Fig. 3A–D) between the mouse groups. Exogenous (diet) lipid retention capacity was tested after oral administration of ^3H -triolein. However, both groups had similar labeled lipid retention capacity in adipose tissue, liver and muscle 24 h after the oral load (Fig. 3E). *De novo* lipid synthesis was examined *in vivo* and in isolated adipocytes (Fig. 3F, G). hCETP and NTg mice showed similar incorporation of $^3\text{H}_2\text{O}$ into lipids of both lipogenic tissues, namely, adipose depots and liver. This method is considered an index of the flux of total precursors converted to fatty acids, independent of the carbon source [31], and is thus ideal for comparing *in vivo* lipogenesis in distinctive tissues (Fig. 3F). Carbon incorporation into lipids was also verified using the ^{14}C -acetate precursor in isolated adipocytes, and no differences in adipose lipogenesis were observed between groups (Fig. 3G).

3.3. CETP expression increases lipolysis and energy expenditure

Considering that hCETP transgenic mice had similar lipid ingestion, excretion, synthesis and retention rates, the reduction in adiposity could be explained by an increase in the lipolysis rates. We used glycerol levels as an indicator of lipolysis since lipolysis-released fatty acids are promptly (re)taken up by tissues [32]. Thus, by measuring plasma and cell media glycerol levels, we verified an increase in basal lipolysis *in vivo* (55%) and in isolated adipocytes (50%) in hCETP-expressing mice and adipose cells, respectively (Fig. 4A, B). In addition, we verified that hCETP-expressing mice exhibit increased whole-body energy expenditure (EE) rates (12%)

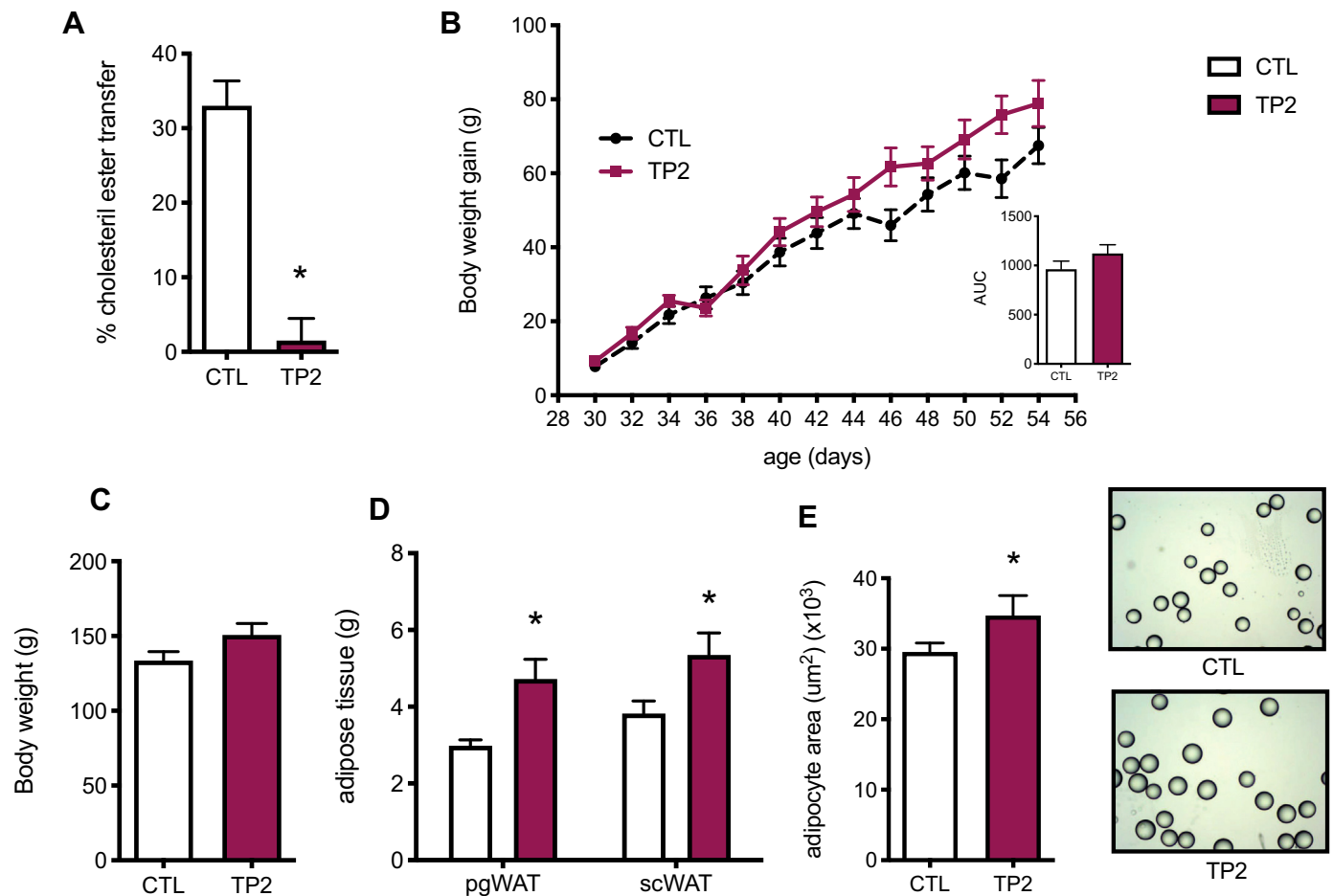


Fig. 2. CETP inhibition increases adiposity in Golden Syrian hamsters. (A) Plasma CETP levels, (B) body weight gain curve and area under the curve (AUC), (C) body and (D) adipose tissue mass (perigonadal: pgWAT, subcutaneous: scWAT) and (E) perigonadal adipocyte size in female Golden Syrian hamsters treated with a neutralizing CETP monoclonal antibody (TP2) or irrelevant IgG (control group) for 1 month. Mean \pm SE ($n = 4-5$). Student's *t*-test, * $p < 0.05$.

(Fig. 4C), measured during the light (morning) period of the day. Increased oxygen consumption and carbon dioxide production in hCETP are shown in Supplementary Fig. S3. In addition, the response of body oxygen consumption to isoproterenol, an indicator of brown adipose tissue activity [33], was 20% higher in hCETP-expressing mice than in NTg mice (Fig. 4D).

Consistent with these data, measurements of mRNA expression in white perigonadal (pWAT) and interscapular brown (iBAT) adipose tissue of hCETP mice showed an increase in lipolytic and thermogenic genes, including adipose triglyceride lipase (ATGL), beta-3 adrenergic receptor (B3AR), hormone sensitive lipase (HSL), and uncoupling protein 1 (UCP1) (Fig. 5A, B). While ATGL is the rate-limiting step for TG hydrolysis in basal lipolysis, HSL is the most important lipase in catecholamine-stimulated lipolysis [34]. Interestingly, fatty acid transport protein 1 (FATP1) mRNA expression was also increased in CETP WAT and BAT, suggesting stimulation of fatty acid (re)uptake (Fig. 5A, B). Protein content analysis confirmed that HSL is increased in both WAT and iBAT of hCETP mice, but the UCP1 protein content was not altered in iBAT (Fig. 5C, D). The plasma levels of lipolytic hormones such as corticosterone, thyroxine, epinephrine and norepinephrine were not elevated in hCETP mice (Fig. S4 A–D), nor was the adipose content of catecholamines (epinephrine and norepinephrine) (Fig. S4 E, F). The expression of genes related to “browning” of white adipose tissue (PR domain containing 16 - PRDM16, cell death inducing DFFA like effector A (Cidea), zinc finger protein 516 (Zfp516) and

peroxisome proliferator-activated receptor gamma coactivator 1-alpha (PGC1a) was not modified in the inguinal WAT of the hCETP mice (Fig. S4 G).

3.4. CETP expression reduces adiposity and increases WAT lipolysis and BAT activity in an independent line of transgenic mice (simian CETP)

To confirm and expand the results described above, we studied another independent CETP transgenic mouse line that expresses simian CETP cDNA (sCETP) under the control of the metallothionein promoter. Similar to hCETP, the body weights of sCETP mice did not differ from those of NTg littermates (Fig. 6A), but sCETP mice showed a reduction in the mass of white adipose tissue depots (Fig. 6B), total body adipose volume (approximately 30%) (Fig. 6C) and leptin plasma level (33%) (Fig. 6D). The spontaneous physical activity was similar in both groups (Fig. 6E). Respiratory analyses also indicated an increase in the energy expenditure rate in sCETP-expressing mice (Fig. 6F). Increased oxygen consumption and carbon dioxide production in sCETP are shown in Supplementary Fig. S3. The *in vivo* lipolysis in sCETP mice was increased in both basal and stimulated (isoproterenol) conditions (Fig. 7A). Although rectal temperature was similar in both groups of mice (Fig. 7B), the maximum temperature of the interscapular area (iBAT temperature) was increased in sCETP-expressing mice (Fig. 7C). The protein levels of phosphorylated HSL (pHSL) are elevated in adipose tissues of sCETP mice (Fig. 7D, E), but iBAT UCP1 is not.

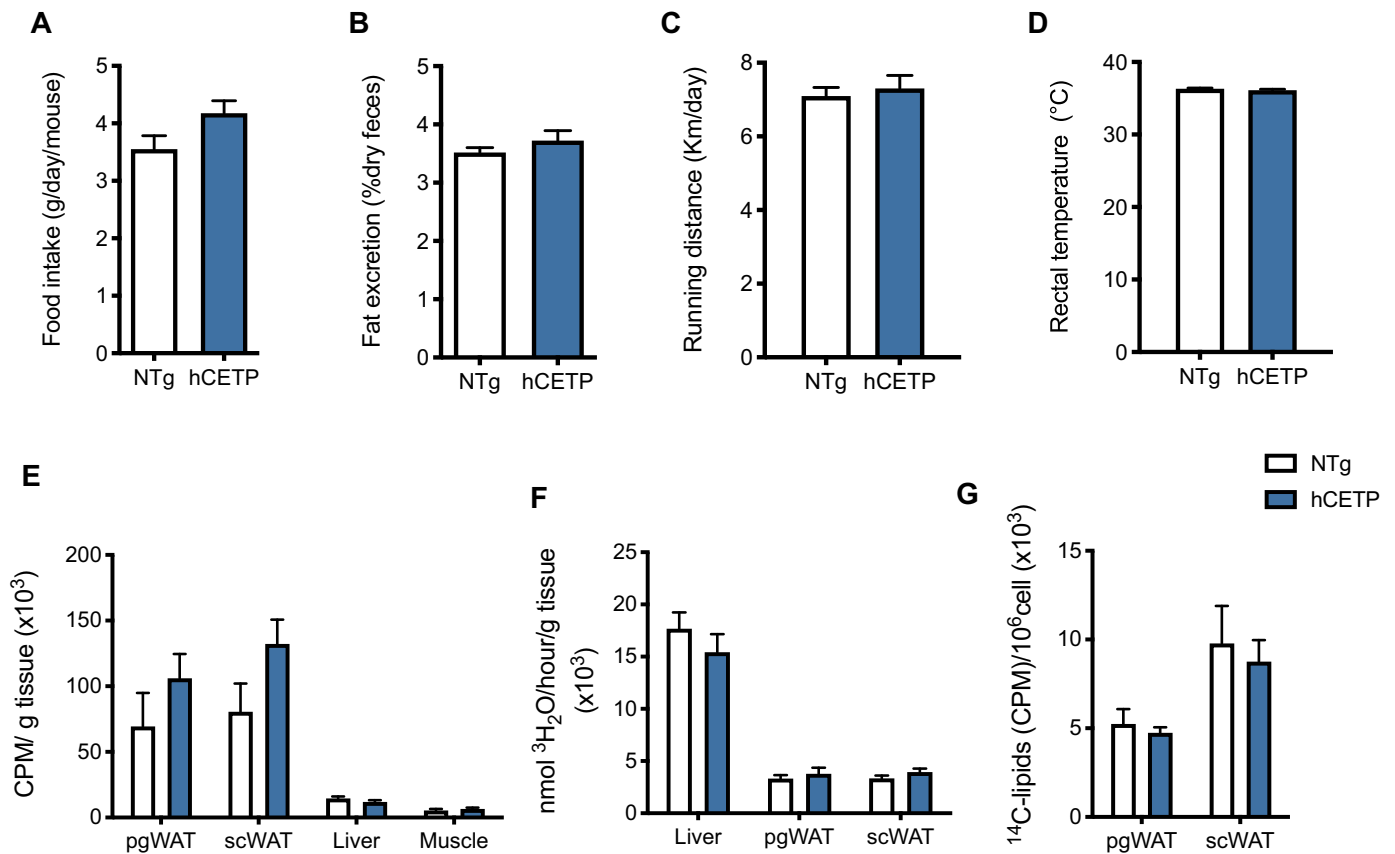


Fig. 3. CETP expression does not affect eating and locomotor behavior, body temperature, lipid retention or lipogenesis. (A) Food intake, (B) fat excretion (% dry feces) in a three-day period ($n = 4$ per group), (C) voluntary physical activity (presence of running wheel) ($n = 5-7$), (D) rectal temperature ($n = 10$), (E) exogenous lipid retention (24 h after an oral dose of ^3H -triolenin in corn oil ($5 \mu\text{Ci } ^3\text{H-TO}$, 180 mg) ($n = 7$), (F) *in vivo* lipogenesis rates estimated by tritiated water ($n = 5-6$), and (G) lipogenesis in isolated adipocytes (10^6 cells, $1 \mu\text{Ci } ^{14}\text{C}$ -acetate, 10 nM acetate, 2 h, 37°C , two independent experiments) ($n = 7$) of nontransgenic (NTg) and human CETP (hCETP) mice. Mean \pm SE. Student's t-test.

To explain the higher iBAT activity, we next investigated UCP1 activity by measuring UCP1-linked respiration in iBAT-isolated mitochondria and the respiration rates of iBAT biopsies. UCP1-linked respiration was measured as the difference between the basal respiration rate and the residual respiration following the addition of a UCP1 inhibitor, GDP. In isolated iBAT mitochondria, no differences were verified between sCETP and NTg mice in basal, maximal and UCP1-linked respiration rates (Fig. 8A); however, the basal oxygen consumption rate of iBAT biopsies was significantly increased (~25%) in the sCETP group (Fig. 8B). These findings show that CETP does not affect UCP1 activity per mitochondrial unit, in agreement with the lack of changes in UCP1 protein expression in iBAT and the similar citrate synthase activity, an indicator of mitochondrial amount, in the iBAT of both groups (120.06 ± 2.29 vs 120.56 ± 3.18 OD₄₁₂/min/mg protein, $n = 6$, sCETP vs NTg, respectively). Thus, the increased oxygen consumption verified in iBAT biopsies of sCETP mice reflects the presence of local stimulating factors *in situ*, likely the lipolysis-derived substrates activating energy consumption and dissipation. These findings suggest that the effect of CETP on increasing body metabolism is mediated, at least in part, by BAT activity (lipolysis, oxygen consumption and heat production).

3.5. Exploring additional mechanisms linking CETP expression with lipolysis and thermogenesis: CETP expression increases iBAT heat production upon cold exposure

Since membrane cholesterol content may regulate energy homeostasis related gene expression [35], we determined total cholesterol

content of pgWAT and iBAT of CETP and NTg mice (Fig. 9). In fact, we found increased cholesterol content in iBAT of hCETP mice but not in sCETP mice. An evaluation of the isolated adipocyte membranes would have been more sensitive.

Bile acids are known regulators of thermogenesis [36]. Thus, we determined total bile acids plasma levels in mice but found no significant differences between CETP and NTg groups (Table 1). However, this finding does not discard the possibility of an elevation of a specific class of bile acids or increased turnover of bile acids in CETP mice.

Yet another possibility was tested, named the macrophage infiltration into adipose tissue. Depending on the amount and type, these cells can induce considerable adipose tissue remodeling through inflammation and lipolysis [37]. However, no differences between groups were found, thus ruling out a possible interference of local inflammation or differential behavior of CETP expressing macrophages within adipose tissue. This is somewhat expected since we are comparing lean (NTg) and leaner (CETP) mice without any pro-inflammatory challenge.

To go deeper into the BAT activity and possible browning of inguinal WAT, we exposed sCETP mice to cold (4°C) for 24 h and followed rectal and iBAT temperature (Fig. 10). We observe that, although leaner, sCETP mice were able to preserve their body temperature within the 24 h similarly to NTg mice (Fig. 10A), meaning that their metabolism is higher enough to sustain body temperature with less insulation. Noteworthy, the iBAT maximal temperature after 24 h of cold exposure was increased in sCETP mice (Fig. 10B). These data indicate that iBAT activity is really higher in CETP expressing mice.

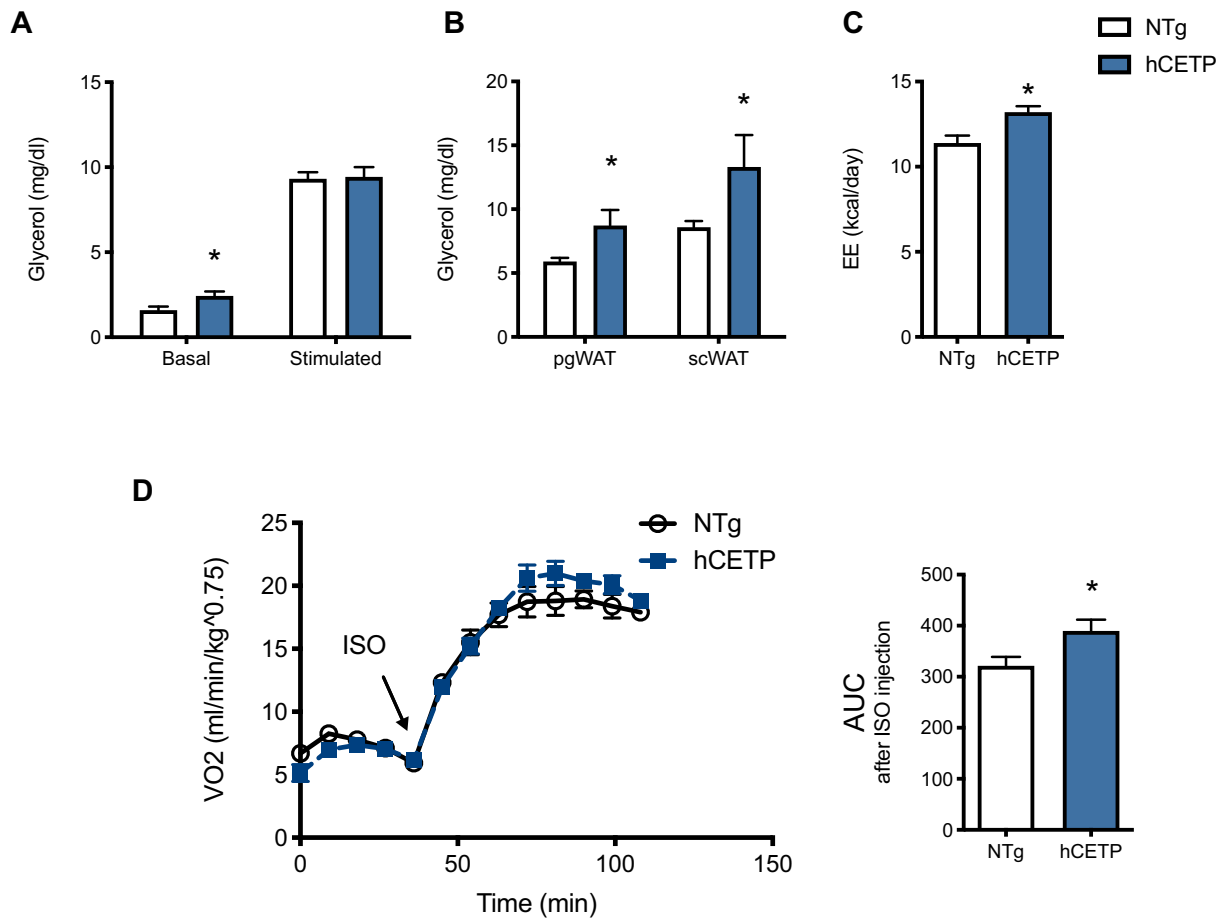


Fig. 4. CETP expression increases lipolysis and energy expenditure. (A) Basal and stimulated lipolysis in the fed state: glycerol levels in plasma before and 15 min after an intraperitoneal injection of isoproterenol (0.3 mg/kg BW) ($n = 6-7$), (B) glycerol release by isolated adipocytes of perigonadal (pgWAT) and subcutaneous (scWAT) adipose tissue (10^6 cells, 0.2 U/mL adenosine deaminase, 10^{-5} M isoproterenol, 1.5 h, 37 °C, $n =$ triplicates, 2–3 mice per pool), (C) whole-body energy expenditure in the fed state, during the morning period ($n = 9-10$), and (D) oxygen consumption in response to isoproterenol (10 mg/kg BW) ($n = 6-5$) in nontransgenic (NTg) and human CETP (hCETP) mice. Mean \pm SE. Student's t-test, * $p \leq 0.05$.

Gene markers of browning of inguinal subcutaneous adipose were not differentially modified (Fig. 10C) in scCETP and NTg after cold exposure.

4. Discussion

Here, we showed that CETP expression reduces body adiposity, revealing a new role of this protein and adding a relevant factor to be considered in the context of obesity. We demonstrated that CETP reduces adiposity without any effect on food intake, fat excretion or physical activity. We also excluded the effect of CETP on *de novo* lipogenesis and on dietary lipid retention capacity. Fatty acid esterification and storage in adipose tissue is limited by glucose uptake, which we previously demonstrated is not disturbed by CETP expression [38]. We also demonstrated that CETP expression increases the WAT and BAT lipolysis rates, body metabolic rate, and iBAT activity. The higher iBAT activity is the most robust finding of this study that contribute to the leaner phenotype observed in the CETP-expressing mice. This was demonstrated by higher local heat production (iBAT temperature) at both 22 and 4 °C environment, higher oxygen consumption *in vivo* (post-isoproterenol stimulation) and *ex-vivo* (high resolution oximetry in iBAT biopsies) and increased expression of lipolysis related genes and proteins.

Some mechanisms to explain how CETP has these adiposity-reducing and thermogenic stimulating effects can be hypothesized.

First, one could think of a central nervous signal to autonomic activation of adipose tissue triggering lipolysis and thermogenesis. We measured the circulating levels and adipose content of catecholamines as indicative of this pathway but found no differences between CETP and NTg mice. Other plasma catabolic hormones, such as thyroid hormones and corticosterone, were also not different between the groups.

An alternative hypothesis is related to the ability of CETP to increase membrane cholesterol content and then indirectly modulate gene expression and/or protein activation, promoting lipolysis and thermogenesis. Accordingly, we detected increased cholesterol content of hCETP iBAT. Our group had already demonstrated that CETP expression increases adipose tissue uptake of cholesterol derived from HDL [12], and others have demonstrated that CETP raises the cholesterol content in adipose cell culture [10,11]. The cholesterol content in adipocyte membranes modifies the expression of several energy metabolism-related genes [35]. In addition, there is evidence that membrane cholesterol [39] and other lipids [40], especially in lipid rafts, are responsible for the stability of beta-adrenergic receptors (B3AR). The activation of B3AR starts lipolysis signaling through protein kinase A phosphorylation of HSL and perilipin [41]. In BAT, B3AR activation promotes both lipolysis and thermogenesis [42]. The present data show that B3AR activated by isoproterenol induced higher lipolysis and oxygen consumption rates in CETP-expressing mice compared to NTg mice. Thus, we could postulate that CETP increases adipocyte cholesterol uptake,

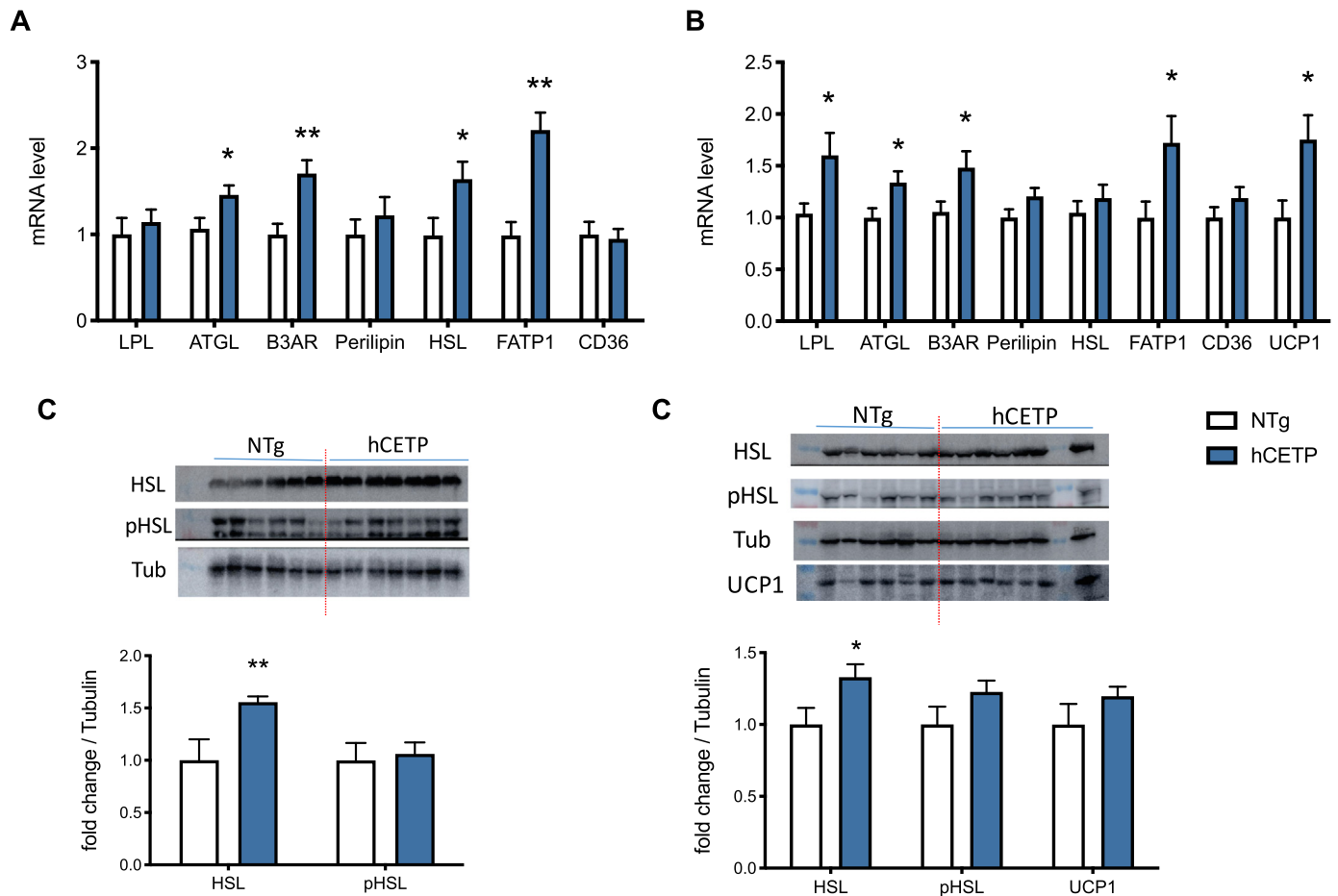


Fig. 5. CETP expression increases lipolysis and thermogenesis-related gene expression. Lipolysis- and thermogenic-related gene expression in (A) perigonadal adipose tissue (pgWAT) and (B) interscapular brown adipose tissue (iBAT) ($n = 8-12$), hormone-sensitive lipase (total and phosphorylated) and UCP1 protein expression in (C) pgWAT and (D) iBAT ($n = 6-7$) of nontransgenic (NTg) and human CETP (hCETP) mice. Mean \pm SE. Student's t-test, * $p \leq 0.05$; ** $p \leq 0.01$.

which stabilizes B3AR and intensifies WAT and BAT lipolysis signaling. We showed that CETP also increases ATGL and HSL expression and activation. The availability of lipolysis-derived NEFAs may increase UCP1 activity or other uncoupling mechanisms resulting in heat production and energy dissipation in BAT. The increased expression of LPL and FATP1 in iBAT are also important for NEFA uptake and further increase mitochondrial uncoupling mechanisms *in situ* and *in vivo*.

Additional hypotheses to explain the impact of CETP on adiposity may still be raised. For instance, elevation of bile acids are known activators of thermogenesis [36]. We did not find higher total circulating steady state levels of bile acids in CETP expressing mice, however, this finding does not discard possible increases of a specific class of bile acids or increased turnover of bile acids [43,44]. In fact, increased bile acid turnover was shown by Cappel et al. [43] in female sCETP mice, stimulating BAT activity *via* TGR5 receptors and iodothyronine deiodinase 2 activity. Finally, considering that CETP may be involved in the modulation of inflammatory and/or redox signaling [45–47], these pathways could also modulate lipid accumulation in adipose tissue [48].

Studies in other animal models support the data presented here. Zhou et al. [49] studied transgenic mice expressing CETP only in adipose tissue, but these mice exhibit physiological levels of plasma CETP. Compared to nontransgenic mice, aP2-CETP transgenic mice had smaller perigonadal adipocytes and reduced expression of adipogenic genes (LPL, PPAR γ and SREBP-1c). Rautureau et al.

[50] showed that CETP expression reversed the phenotype of increased whole-body adipose tissue volume observed in adenylate cyclase 9 inactivated mice. Intriguingly, Cappel et al. [43] studied the same sCETP mice used here and reported no changes in global adiposity, as measured by NMR. Differences in methodology or in the strain background may explain these dissimilar results. We studied hCETP and sCETP in the C57BL6/JUnib background with preserved nicotinamide nucleotide transhydrogenase (NNT) expression, a mitochondrial enzyme that is mutated in C57BL6/J mice from the Jackson Laboratory. This NNT mutation has been associated with impaired glucose tolerance [51], susceptibility to obesity [52], fatty liver [53] and atherosclerosis [54].

Interestingly, in *C. elegans*, the inhibition of an orthologous CETP gene (ZC513.1) results in increased fat content [55], as we observed in hamsters with inhibition of CETP. In agreement with our results of stimulated lipolysis in CETP mice, Izem et al. [13] showed that overexpression of CETP in human liposarcoma cells (SW872) increased TG hydrolysis by 2.6 times and reduced TG accumulation and synthesis by 50% and 26%, respectively.

Some human studies support the association of CETP with adiposity reduction. Subjects with reduced plasma CETP activity due to the CETP polymorphism I405V showed a greater increase in visceral adipose mass (130%) after overfeeding [56]. The same CETP polymorphism screened in 295 eutrophic subjects showed an association of reduced CETP activity with elevated body mass index (BMI) and waist circumference [46]. According to Johansson et al. [57], obese subjects showed

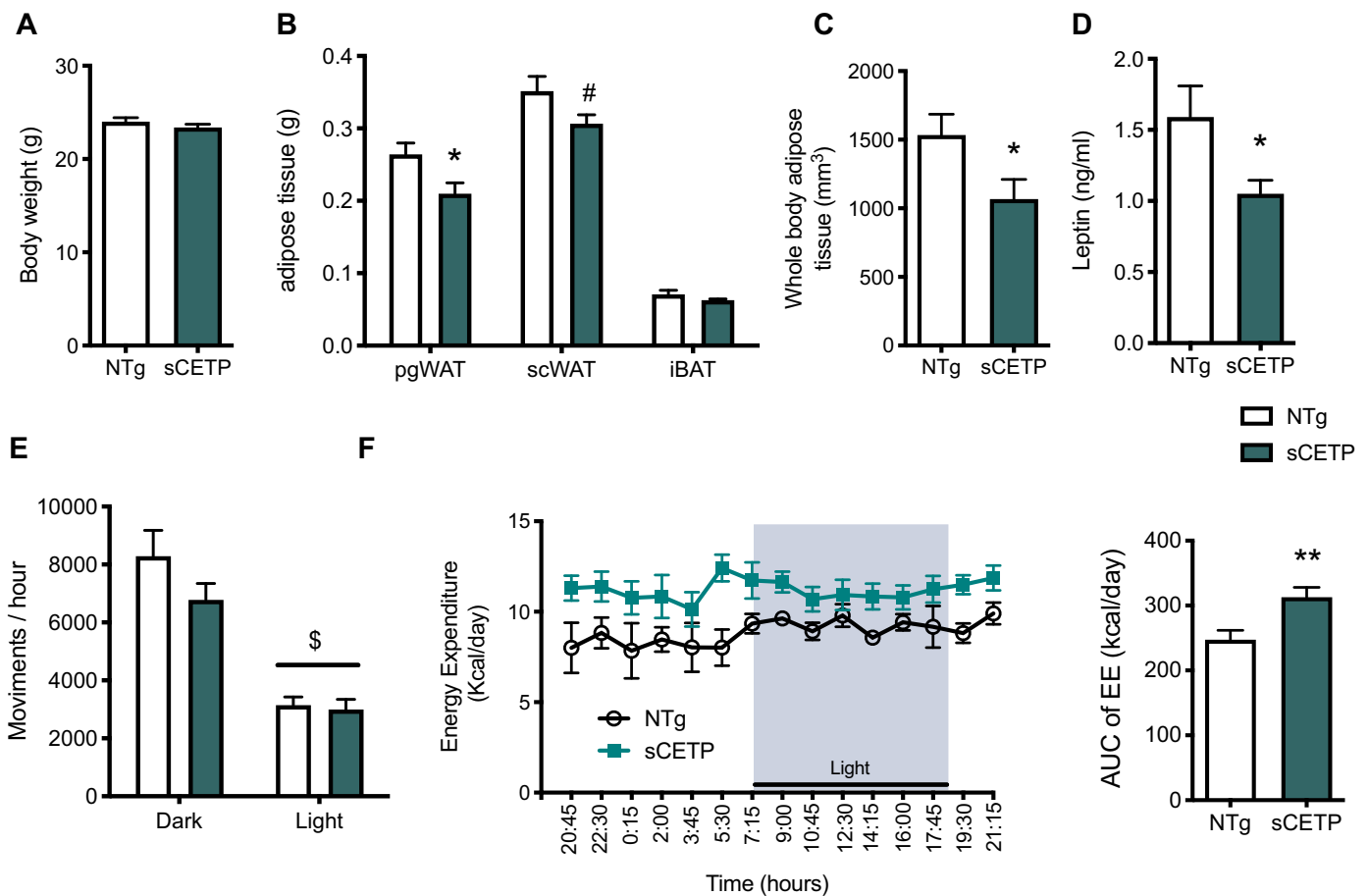


Fig. 6. CETP expression also reduces adiposity in an independent strain of mice (sCETP). (A) Body and (B) adipose tissue mass (pgWAT, perigonadal; scWAT, subcutaneous and iBAT, interscapular brown adipose tissue) ($n = 5-7$), (C) whole-body adipose tissue volume: CT scan ($n = 5-7$), (D) leptin plasma level ($n = 4-5$), (E) spontaneous activity (all movements) ($n = 6$), and (F) whole-body energy expenditure (24 h) ($n = 5-7$) of nontransgenic (NTg) and simian CETP (sCETP) mice. Mean \pm SE. Student's *t*-test, sCETP vs. NTg * $p \leq 0.05$; ** $p \leq 0.01$; # $p \leq 0.07$. Two-way ANOVA, dark vs. light \$ $p \leq 0.0001$.

increased CETP expression along with weight loss. On the other hand, studies point to the opposite direction. For the -629C/A polymorphism, CETP levels were higher in patients with metabolic syndrome than in the healthy group [58]. The D442G mutation of the CETP gene that leads to reduced CETP mass and activity [59] was associated with protection against metabolic syndrome [60]. A comparison between normal-weight and abdominally obese men showed a positive correlation of plasma CE transfer activity with BMI and the waist-to-hip ratio [61]. Thus, studies in human populations are quite complex because of relevant differences in the metabolic context, such as insulin sensitivity, genetic background and epigenetic phenomena. Two independent groups studied the interaction between epigenetics and obesity/adiposity, evaluating the DNA methylation pattern specifically in adipose tissue. They highlighted the CETP gene methylation pattern as a marker of types of obesity (android/central vs. gynoid) [62] and as a marker of weight loss response after surgical intervention [63]. A recent cohort of Spanish children and adolescents identified the CETP polymorphism (rs708272-CETP) among the top ten single nucleotide polymorphisms that are important for predicting overweight-obesity [64].

5. Conclusion

In summary, by comparing all or none (mice) and high and low (hamsters) CETP-expressing models, under genetic homogeneous backgrounds, we were able to show that CETP stimulates lipolysis and thermogenesis, increasing body energy expenditure and

promoting a significant reduction in body fat. These findings indicate a new anti-adipogenic role for CETP, highlighting a relevant factor to be considered in the context of obesity.

Funding

This work was supported by grants from Fundação de Amparo à Pesquisa do Estado de São Paulo: #2013/07607-8 and #2017/17728-8 (to HCFO) and the following fellowships: #2015/17555-0 (to HFR), #2015/07670-7 (to BC), #2019-02340-0 (to JZC) and Conselho Nacional de Desenvolvimento Científico e Tecnológico (CNPq, #300937/2018-0 to HCFO).

CRedit authorship contribution statement

HFR participated in the study design, data acquisition and interpretation and manuscript writing. JZC carried out the indirect calorimetry and body temperature and cold exposure experiments. PRP carried out hamster experiments. BC carried out mitochondria and BAT oxygen consumption experiments. PMMV carried out adipose tissue macrophage flow cytometry analysis. VSN carried out gas chromatography/mass spectrometry analysis. HCFO is responsible for project conception, study design, data interpretation, manuscript writing and grants. All authors read and approved the final manuscript.

Declaration of competing interest

None.

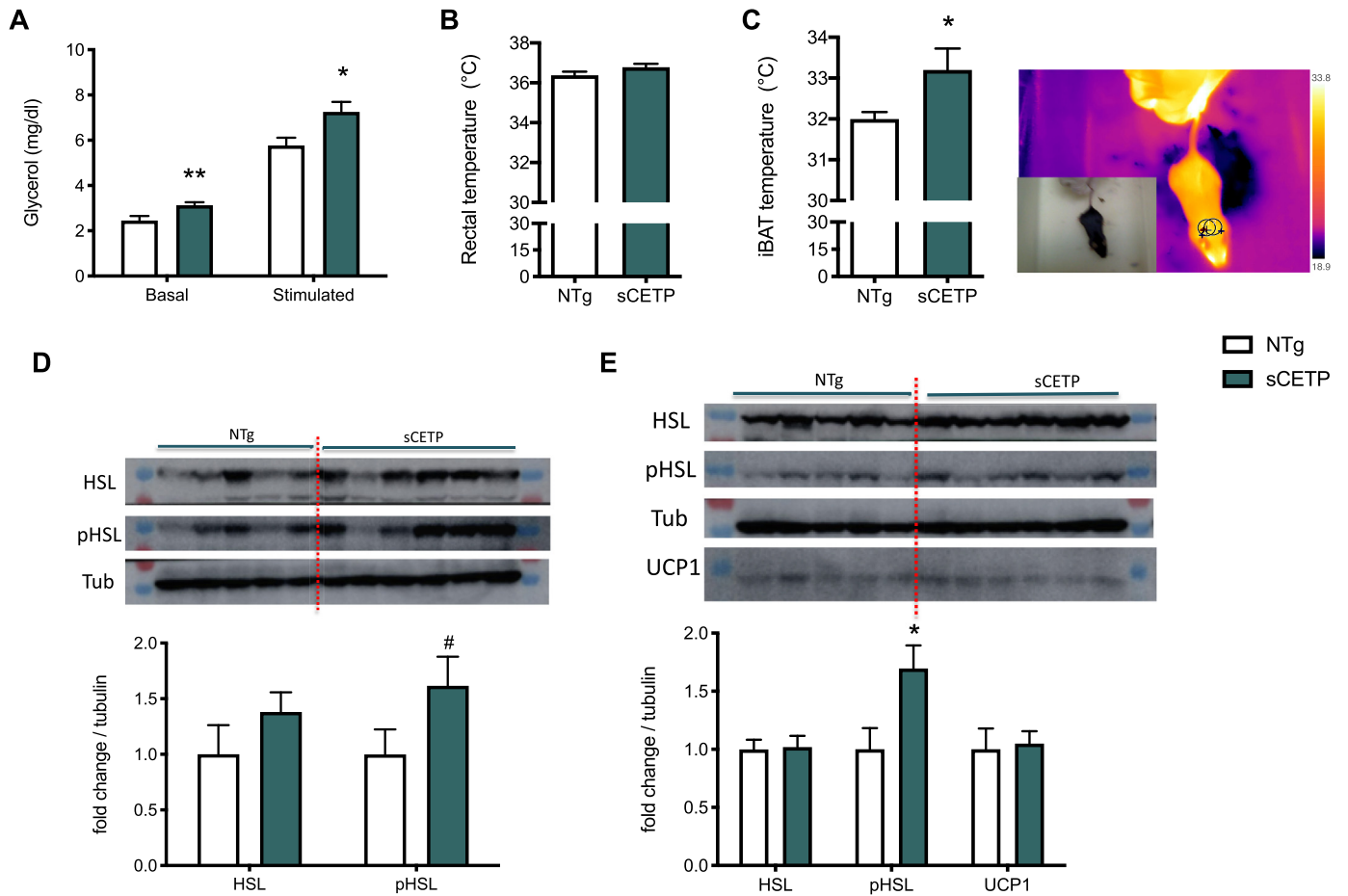


Fig. 7. CETP expression increases lipolysis and BAT temperature in an independent strain of mice (sCETP). (A) Basal and stimulated lipolysis in the fed state (n = 6–7): glycerol levels in plasma before and 15 min after an intraperitoneal injection of isoproterenol (0.3 mg/kg BW); (B) rectal body temperature (n = 6); (C) iBAT maximum temperature: infrared camera (n = 7–10); total and phosphorylated hormone sensitive lipase (HSL) and UCP1 protein expression in (D) perigonadal adipose tissue: pgWAT and (E) interscapular brown adipose tissue: iBAT (n = 5–6) of nontransgenic (NTg) and simian CETP (sCETP) mice. Mean ± SE. Student's t-test, *p < 0.05; #p = 0.057.

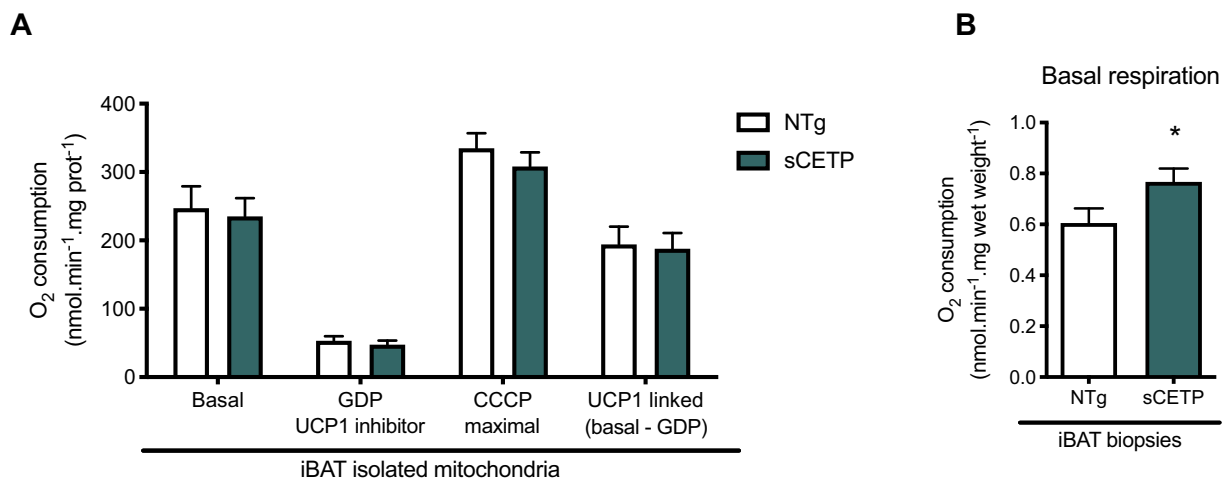


Fig. 8. CETP expression increases BAT oxygen consumption. (A) Oxygen consumption rates of isolated mitochondria from interscapular brown adipose tissue (iBAT): basal respiration, residual respiration following GDP addition (UCP1 inhibitor, 1 μM), maximal oxygen consumption (induced by CCCP, 5 μM) and UCP1 linked respiration (basal - GDP), and (B) basal oxygen consumption of iBAT biopsies of nontransgenic (NTg) and simian CETP (sCETP) mice. Mean ± SE (n = 8–9). Student's t-test, *p < 0.05.

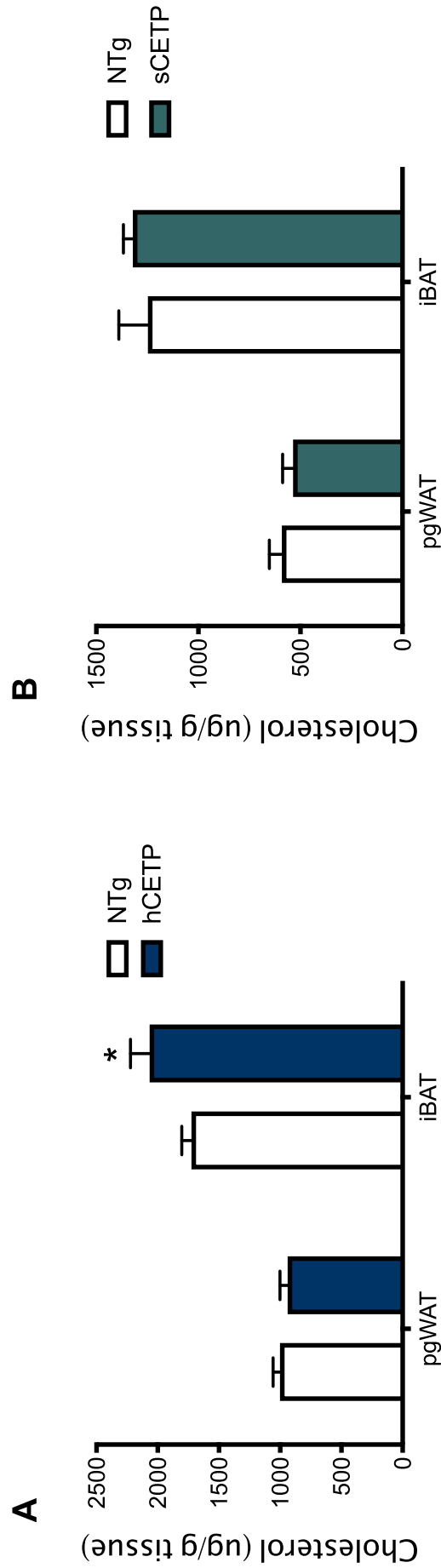


Fig. 9. CETP expression increases cholesterol content in iBAT. Total cholesterol content in perigonadal white adipose tissue (pgWAT) and interscapular brown adipose tissue (iBAT) of human CETP (hCETP, n = 10) (A) and simian CETP (sCETP, n = 6-10) (B) mice versus nontransgenic (NTg) controls. Mean \pm SE. Student's t-test, * $p \leq 0.05$.

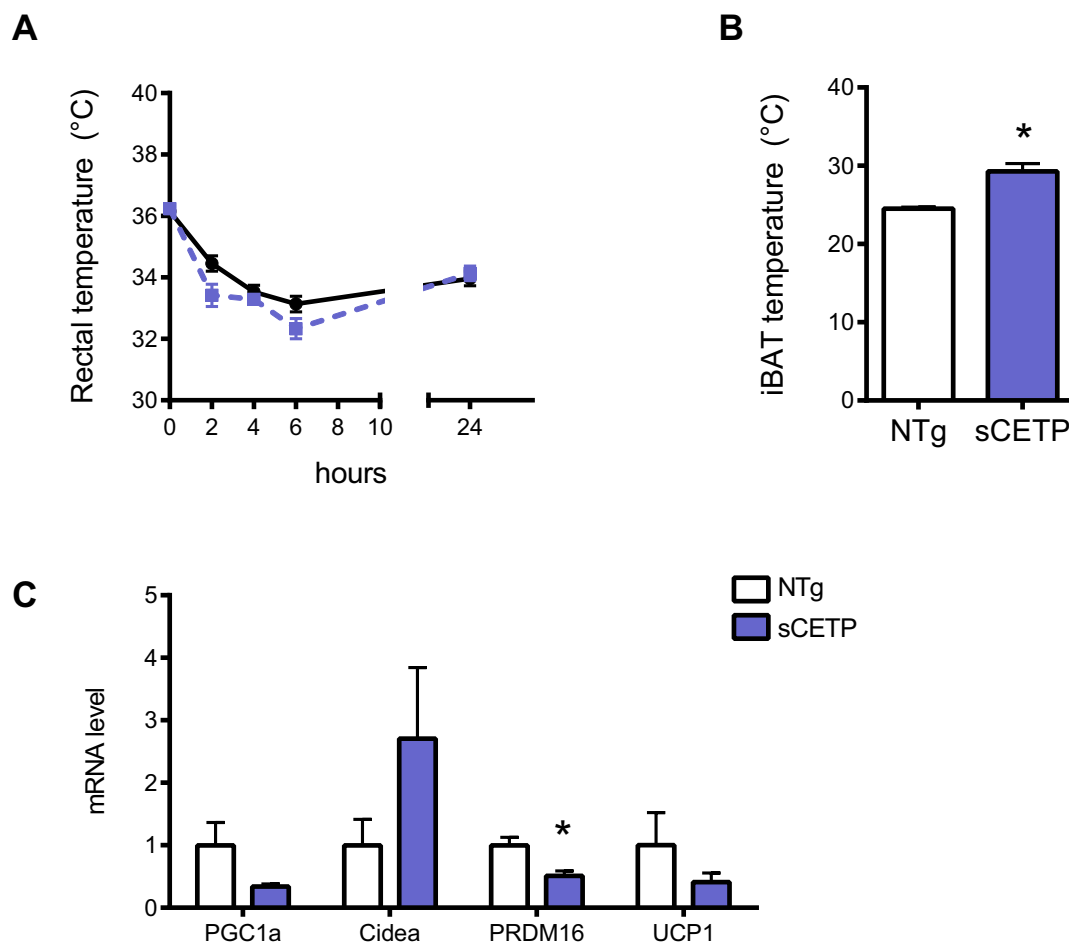


Fig. 10. CETP expressing mice exposed to cold sustain their body temperature and increases iBAT temperature. (A) Rectal temperature during 24 h at 4 °C; (B) interscapular temperature (iBAT region); (C) inguinal subcutaneous adipose tissue (scWAT) expression of browning related genes after 7 days of exposure to 4 °C. Mean \pm SE (n = 5–6). Student's t-test, * $p < 0.05$.

Acknowledgments

We are grateful for the technical assistance of Janaína Christovam, Juliana C. Rovani, Adriene A. Paiva, Gabriel G. Dorighello, and Carolina M. Lazaro. We also thank Professor Anibal E. Vercesi for helping with BAT mitochondrial respiration protocols and laboratory facilities.

Appendix A. Supplementary data

Supplementary data to this article can be found online at <https://doi.org/10.1016/j.metabol.2020.154429>.

References

- Drayna D, Jarnagin AS, McLean J, Henzel W, Kohr W, Fielding C, et al. Cloning and sequencing of human cholesteryl ester transfer protein cDNA. *Nature*. 1987;327(6123):632–4. <https://doi.org/10.1038/327632a0>.
- Ha YC, Barter PJ. Differences in plasma cholesteryl ester transfer activity in sixteen vertebrate species. *Comp Biochem Physiol B*. 1982;71(2):265–9. [https://doi.org/10.1016/0305-0491\(82\)90252-8](https://doi.org/10.1016/0305-0491(82)90252-8).
- Tsutsumi K, Hagi A, Inoue Y. The relationship between plasma high density lipoprotein cholesterol levels and cholesteryl ester transfer protein activity in six species of healthy experimental animals. *Biol Pharm Bull*. 2001;24(5):579–81. <https://doi.org/10.1248/bpb.24.579>.
- Radeau T, Lau P, Robb M, McDonnell M, Ailhaud G, McPherson R. Cholesteryl ester transfer protein (CETP) mRNA abundance in human adipose tissue: relationship to cell size and membrane cholesterol content. *J Lipid Res*. 1995;36(12):2552–61.
- Tall AR. Plasma cholesteryl ester transfer protein. *J Lipid Res*. 1993;34(8):1255–74.
- Barter PJ, Caulfield M, Eriksson M, Grundy SM, Kastelein JJP, Komajda M, et al. Effects of torcetrapib in patients at high risk for coronary events. *N Engl J Med*. 2007;357(21):2109–22. <https://doi.org/10.1056/NEJMoa0706628>.
- Schwartz GG, Olsson AG, Abt M, Ballantyne CM, Barter PJ, Brumm J, et al. Effects of dalcetrapib in patients with a recent acute coronary syndrome. *N Engl J Med*. 2012;367(22):2089–99. <https://doi.org/10.1056/NEJMoa1206797>.
- Lincoff AM, Nicholls SJ, Riesmeyer JS, Barter PJ, Brewer HB, Fox KAA, et al. Evacetrapib and cardiovascular outcomes in high-risk vascular disease. *N Engl J Med*. 2017;376(20):1933–42. <https://doi.org/10.1056/NEJMoa1609581>.
- Bowman L, Hopewell JC, Chen F, Wallendszus K, Stevens W, et al. HPS3/TIMI55-REVEAL Collaborative Group. Effects of Anacetrapib in patients with atherosclerotic vascular disease. *N Engl J Med*. 2017;377(13):1217–27. <https://doi.org/10.1056/NEJMoa1706444>.
- Oliveira HCF, Raposo HF. Cholesteryl Ester transfer protein and lipid metabolism and cardiovascular diseases. In: Jiang X-C, editor. *Lipid transfer in lipoprotein metabolism and cardiovascular disease*. Singapore: Springer; 2020. p. 15–25.
- Benoist F, Lau P, McDonnell M, Doelle H, Milne R, McPherson R. Cholesteryl Ester transfer protein mediates selective uptake of high density lipoprotein Cholesteryl esters by human adipose tissue. *J Biol Chem*. 1997;272(38):23572–7. <https://doi.org/10.1074/jbc.272.38.23572>.
- Harada LM, Amigo L, Cazita PM, Salerno AG, Rigotti AA, Quintão ECR, et al. CETP expression enhances liver HDL-cholesteryl ester uptake but does not alter VLDL and biliary lipid secretion. *Atherosclerosis*. 2007;191(2):313–8. <https://doi.org/10.1016/j.atherosclerosis.2006.05.036>.
- Izem L, Greene DJ, Bialkowska K, Morton RE. Overexpression of full-length cholesteryl ester transfer protein in SW872 cells reduces lipid accumulation. *J Lipid Res*. 2015;56(3):515–25. <https://doi.org/10.1194/jlr.M053678>.
- Wang J, Perrard XD, Perrard JL, Mukherjee A, Rosales C, Chen Y, et al. ApoE and the role of very low density lipoproteins in adipose tissue inflammation. *Atherosclerosis*. 2012;223(2):342–9. <https://doi.org/10.1016/j.atherosclerosis.2012.06.003>.
- Li Y-H, Liu L. Apolipoprotein E synthesized by adipocyte and apolipoprotein E carried on lipoproteins modulate adipocyte triglyceride content. *Lipids Health Dis*. 2014;13:136. <https://doi.org/10.1186/1476-511X-13-136>.
- Raposo HF, Paiva AA, Kato LS, de Oliveira HCF. Apolipoprotein CIII overexpression exacerbates diet-induced obesity due to adipose tissue higher exogenous lipid uptake and retention and lower lipolysis rates. *Nutr Metab*. 2015;12:61. <https://doi.org/10.1186/s12986-015-0058-6>.

- [17] Salerno AG, Silva TR, Amaral MEC, Alberici LC, Bonfleur ML, Patrício PR, et al. Overexpression of apolipoprotein CIII increases and CETP reverses diet-induced obesity in transgenic mice. *Int J Obes* (2005). 2007;31(10):1586–95. <https://doi.org/10.1038/sj.ijo.0803646>.
- [18] Jiang XC, Agellon LB, Walsh A, Breslow JL, Tall A. Dietary cholesterol increases transcription of the human cholesteryl ester transfer protein gene in transgenic mice. Dependence on natural flanking sequences. *J Clin Invest*. 1992;90(4):1290–5. <https://doi.org/10.1172/JCI115993>.
- [19] Marotti KR, Castle CK, Boyle TP, Lin AH, Murray RW, Melchior GW. Severe atherosclerosis in transgenic mice expressing simian cholesteryl ester transfer protein. *Nature*. 1993;364(6432):73–5. <https://doi.org/10.1038/364073a0>.
- [20] Oliveira HC, Ma L, Milne R, Marcovina SM, Inazu A, Mabuchi H, et al. Cholesteryl ester transfer protein activity enhances plasma cholesteryl ester formation. Studies in CETP transgenic mice and human genetic CETP deficiency. *Arterioscler Thromb Vasc Biol*. 1997;17(6):1045–52. <https://doi.org/10.1161/01.atv.17.6.1045>.
- [21] Hildebrandt AL, Kelly-Sullivan DM, Black SC. Validation of a high-resolution X-ray computed tomography system to measure murine adipose tissue depot mass in situ and longitudinally. *J Pharmacol Toxicol Methods*. 2002;47(2):99–106. [https://doi.org/10.1016/s1056-8719\(02\)00208-3](https://doi.org/10.1016/s1056-8719(02)00208-3).
- [22] Rodbell M. Metabolism of isolated fat cells. I Effects of hormones on glucose metabolism and lipolysis. *J Biol Chem*. 1964;239:375–80.
- [23] Osuga J, Ishibashi S, Oka T, Yagyu H, Tozawa R, Fujimoto A, et al. Targeted disruption of hormone-sensitive lipase results in male sterility and adipocyte hypertrophy, but not in obesity. *Proc Natl Acad Sci U S A*. 2000;97(2):787–92. <https://doi.org/10.1073/pnas.97.2.787>.
- [24] Osono Y, Woollett LA, Herz J, Dietschy JM. Role of the low density lipoprotein receptor in the flux of cholesterol through the plasma and across the tissues of the mouse. *J Clin Invest*. 1995;95(3):1124–32. <https://doi.org/10.1172/JCI117760>.
- [25] Shepherd D, Garland PB. The kinetic properties of citrate synthase from rat liver mitochondria. *Biochem J*. 1969;114(3):597–610. <https://doi.org/10.1042/bj1140597>.
- [26] Shabalina IG, Ost M, Petrovic N, Vrbacky M, Nedergaard J, Cannon B. Uncoupling protein-1 is not leaky. *Biochim Biophys Acta Bioenerg*. 2010;1797(6):773–84. <https://doi.org/10.1016/j.bbabi.2010.04.007>.
- [27] Hütter E, Unterluggauer H, Garedeu A, Jansen-Dürr P, Gnaiger E. High-resolution respirometry—a modern tool in aging research. *Exp Gerontol*. 2006;41(1):103–9. <https://doi.org/10.1016/j.exger.2005.09.011>.
- [28] Magdalon J, Chimin P, Belchior T, Neves RX, Vieira-Lara MA, Andrade ML, et al. Constitutive adipocyte mTORC1 activation enhances mitochondrial activity and reduces visceral adiposity in mice. *Biochim Biophys Acta*. 2016;1861(5):430–8. <https://doi.org/10.1016/j.bbali.2016.02.023>.
- [29] Moraes-Vieira PM, Castoldi A, Aryal P, Wellenstein K, Peroni OD, Kahn BB. Antigen presentation and T-cell activation are critical for RBP4-induced insulin resistance. *Diabetes*. 2016;65(5):1317–27. <https://doi.org/10.2337/db15-1696>.
- [30] Nunes VS, Leanza CC, Panzoldo NB, Parra E, Cazita PM, Nakandakare ER, et al. HDL-C concentration is related to markers of absorption and of cholesterol synthesis: study in subjects with low vs. high HDL-C. *Clin Chim Acta*. 2011;412(1–2):176–80. <https://doi.org/10.1016/j.cca.2010.09.039>.
- [31] Saggerson ED, McAllister TW, Baht HS. Lipogenesis in rat brown adipocytes. Effects of insulin and noradrenaline, contributions from glucose and lactate as precursors and comparisons with white adipocytes. *Biochem J*. 1988;251(3):701–9.
- [32] Vaughan M. The production and release of glycerol by adipose tissue incubated in vitro. *J Biol Chem*. 1962;237:3354–8.
- [33] Cannon B, Nedergaard J. Nonshivering thermogenesis and its adequate measurement in metabolic studies. *J Exp Biol*. 2011;214(Pt 2):242–53. <https://doi.org/10.1242/jeb.050989>.
- [34] Langin D. Adipose tissue lipolysis as a metabolic pathway to define pharmacological strategies against obesity and the metabolic syndrome. *Pharmacol Res*. 2006;53(6):482–91. <https://doi.org/10.1016/j.phrs.2006.03.009>.
- [35] Lay SL, Krief S, Farnier C, Lefrère I, Liepvre XL, Bazin R, et al. Cholesterol, a cell size-dependent signal that regulates glucose metabolism and gene expression in adipocytes. *J Biol Chem*. 2001;276(20):16904–10. <https://doi.org/10.1074/jbc.M010955200>.
- [36] Watanabe M, Houten SM, Matakai C, Cristoffolete MA, Kim BW, Sato H, et al. Bile acids induce energy expenditure by promoting intracellular thyroid hormone activation. *Nature*. 2006;439(7075):484–9. <https://doi.org/10.1038/nature04330>.
- [37] Ferrante AW. The immune cells in adipose tissue. *Diabetes Obes Metab*. 2013;15(Suppl. 3):34–8. <https://doi.org/10.1111/dom.12154>.
- [38] Raposo HF, Vanzela EC, Berti JA, Oliveira HCF. Cholesteryl ester transfer protein (CETP) expression does not affect glucose homeostasis and insulin secretion: studies in human CETP transgenic mice. *Lipids Health Dis*. 2016;15:9. <https://doi.org/10.1186/s12944-016-0179-6>.
- [39] Cherezov V, Rosenbaum DM, Hanson MA, Rasmussen SGF, Thian FS, Kobilka TS, et al. High-resolution crystal structure of an engineered human beta2-adrenergic G protein-coupled receptor. *Science* (New York, NY). 2007;318(5854):1258–65. <https://doi.org/10.1126/science.1150577>.
- [40] Yao Z, Kobilka B. Using synthetic lipids to stabilize purified beta2 adrenoceptor in detergent micelles. *Anal Biochem*. 2005;343(2):344–6. <https://doi.org/10.1016/j.ab.2005.05.002>.
- [41] Holm C. Molecular mechanisms regulating hormone-sensitive lipase and lipolysis. *Biochem Soc Trans*. 2003;31(6):1120–4. <https://doi.org/10.1042/bst0311120>.
- [42] Zhao J, Unelius L, Bengtsson T, Cannon B, Nedergaard J. Coexisting beta-adrenoceptor subtypes: significance for thermogenic process in brown fat cells. *Am J Physiol*. 1994;267(4 Pt 1):C969–79. <https://doi.org/10.1152/ajpcell.1994.267.4.C969>.
- [43] Cappel DA, Palmisano BT, Emfinger CH, Martinez MN, McGuinness OP, Stafford JM. Cholesteryl ester transfer protein protects against insulin resistance in obese female mice. *Mol Metab*. 2013;2(4):457–67. <https://doi.org/10.1016/j.molmet.2013.08.007>.
- [44] Broeders EPM, Nascimento EBM, Havekes B, Brans B, Roumans KHM, Tailleux A, et al. The bile acid chenodeoxycholic acid increases human brown adipose tissue activity. *Cell Metab*. 2015;22(3):418–26. <https://doi.org/10.1016/j.cmet.2015.07.002>.
- [45] Haas JT, Staels B. Cholesteryl-ester transfer protein (CETP): a Kupffer cell marker linking hepatic inflammation with atherogenic dyslipidemia? *Hepatology*. 2015;62(6):1659–61. <https://doi.org/10.1002/hep.28125>.
- [46] Oliveira HCF, de Faria EC. Cholesteryl ester transfer protein: the controversial relation to atherosclerosis and emerging new biological roles. *IUBMB Life*. 2011;63(4):248–57. <https://doi.org/10.1002/iub.448>.
- [47] Cazita PM, Barbeiro DF, Moretti AIS, Quintão ECR, Soriano FG. Human cholesteryl ester transfer protein expression enhances the mouse survival rate in an experimental systemic inflammation model: a novel role for CETP. *Shock* (Augusta, Ga). 2008;30(5):590–5. <https://doi.org/10.1097/SHK.0b013e31816e30fd>.
- [48] Masschelin PM, Cox AR, Chemis N, Hartig SM. The impact of oxidative stress on adipose tissue energy balance. *Front Physiol*. 2019;10:1638. <https://doi.org/10.3389/fphys.2019.01638>.
- [49] Zhou H, Li Z, Hojjati MR, Jang D, Beyer TP, Cao G, et al. Adipose tissue-specific CETP expression in mice: impact on plasma lipoprotein metabolism. *J Lipid Res*. 2006;47(9):2011–9. <https://doi.org/10.1194/jlr.M600153-JLR200>.
- [50] Rautureau Y, Deschambault V, Higgins M-È, Rivas D, Mecteau M, Geoffroy P, et al. ADCY9 (Adenylate Cyclase type 9) inactivation protects from atherosclerosis only in the absence of CETP (Cholesteryl Ester transfer protein). *Circulation*. 2018;138(16):1677–92. <https://doi.org/10.1161/CIRCULATIONAHA.117.031134>.
- [51] Toye AA, Lippiat JD, Proks P, Shimomura K, Bentley L, Hugill A, et al. A genetic and physiological study of impaired glucose homeostasis control in C57BL/6J mice. *Diabetologia*. 2005;48(4):675–86. <https://doi.org/10.1007/s00125-005-1680-z>.
- [52] Nicholson A, Reifsnnyder PC, Malcolm RD, Lucas CA, MacGregor GR, Zhang W, et al. Diet-induced obesity in two C57BL/6 substrains with intact or mutant nicotinamide nucleotide transhydrogenase (Nnt) gene. *Obesity* (Silver Spring, MD). 2010;18(10):1902–5. <https://doi.org/10.1038/oby.2009.477>.
- [53] Navarro CDC, Figueira TR, Francisco A, Dal'Ó GA, Ronchi JA, Rovani JC, et al. Redox imbalance due to the loss of mitochondrial NAD(P)-transhydrogenase markedly aggravates high fat diet-induced fatty liver disease in mice. *Free Radic Biol Med*. 2017;113:190–202. <https://doi.org/10.1016/j.freeradbiomed.2017.09.026>.
- [54] Salerno AG, Rentz T, Dorigheo GG, Marques AC, Lorza-Gil E, Wanschel ACBA, et al. Lack of mitochondrial NAD(P)-transhydrogenase expression in macrophages exacerbates atherosclerosis in hypercholesterolemic mice. *Biochem J*. 2019;476(24):3769–89. <https://doi.org/10.1042/BJC20190543>.
- [55] Ashrafi K, Chang FY, Watts JL, Fraser AG, Kamath RS, Ahringer J, et al. Genome-wide RNAi analysis of *Caenorhabditis elegans* fat regulatory genes. *Nature*. 2003;421(6920):268–72. <https://doi.org/10.1038/nature01279>.
- [56] Terán-García M, Després J-P, Tremblay A, Bouchard C. Effects of cholesterol ester transfer protein (CETP) gene on adiposity in response to long-term overfeeding. *Atherosclerosis*. 2008;196(1):455–60. <https://doi.org/10.1016/j.atherosclerosis.2006.12.005>.
- [57] Johansson LE, Danielsson APH, Parikh H, Klintonberg M, Norström F, Groop L, et al. Differential gene expression in adipose tissue from obese human subjects during weight loss and weight maintenance. *Am J Clin Nutr*. 2012;96(1):196–207. <https://doi.org/10.3945/ajcn.111.020578>.
- [58] Akbarzadeh M, Hassanzadeh T, Saidijam M, Esmaeili R, Borzouei S, Hajilooi M, et al. Cholesteryl ester transfer protein (CETP)-629C/A polymorphism and its effects on the serum lipid levels in metabolic syndrome patients. *Mol Biol Rep*. 2012;39(10):9529–34. <https://doi.org/10.1007/s11033-012-1817-3>.
- [59] Takahashi K, Jiang XC, Sakai N, Yamashita S, Hirano K, Bujo H, et al. A missense mutation in the cholesteryl ester transfer protein gene with possible dominant effects on plasma high density lipoproteins. *J Clin Invest*. 1993;92(4):2060–4. <https://doi.org/10.1172/JCI116802>.
- [60] Lee H-S, Kim Y, Park T. New common and rare variants influencing metabolic syndrome and its individual components in a Korean population. *Sci Rep*. 2018;8(1):5701. <https://doi.org/10.1038/s41598-018-23074-2>.
- [61] Talbot CPJ, Plat J, Joris PJ, Konings M, Kusters YHAM, Schalkwijk CG, et al. HDL cholesterol efflux capacity and cholesteryl ester transfer are associated with body mass, but are not changed by diet-induced weight loss: a randomized trial in abdominally obese men. *Atherosclerosis*. 2018;274:23–8. <https://doi.org/10.1016/j.atherosclerosis.2018.04.029>.
- [62] Agha G, Houseman EA, Kelsey KT, Eaton CB, Buka SL, Loucks EB. Adiposity is associated with DNA methylation profile in adipose tissue. *Int J Epidemiol*. 2015;44(4):1277–87. <https://doi.org/10.1093/ije/dyu236>.
- [63] Benton MC, Johnstone A, Eccles D, Harmon B, Hayes MT, Lea RA, et al. An analysis of DNA methylation in human adipose tissue reveals differential modification of obesity genes before and after gastric bypass and weight loss. *Genome Biol*. 2015;16:8. <https://doi.org/10.1186/s13059-014-0569-x>.
- [64] Cortés-Martín A, Colmenarejo G, Selma MV, Espín JC. Genetic polymorphisms, Mediterranean diet and microbiota-associated Urolithin Metabotypes can predict obesity in childhood-adolescence. *Sci Rep*. 2020;10(1):7850. <https://doi.org/10.1038/s41598-020-64833-4>.